Theoretical and Applied Mechanics Letters 11 (2021) 100299

Contents lists available at ScienceDirect

Theoretical and Applied Mechanics Letters

journal homepage: www.elsevier.com/locate/taml

Detection of mechanical stress in the steel structure of a bridge crane

Leopold Hrabovský[a,*], Daniel Čepica[b], Karel Frydrýšek[b]

[a] VSB-Technical university of Ostrava, Faculty of mechanical Engineering, Institute of Transport, 17. listopadu 2172/15, 708 00, Ostrava - Poruba, Czech Republic

[b] VSB-Technical university of Ostrava, Faculty of Mechanical Engineering, Department of Applied Mechanics, Ostrava - Poruba, Czech Republic

ARTICLE INFO

Article history:
Received 27 August 2021
Revised 17 September 2021
Accepted 27 September 2021
Available online 1 October 2021

Keywords:
Crane skewing
Mechanical stress detector
Mechanical stress
FEM
Overhead crane

ABSTRACT

A significant negative aspect in the operation of bridge-type cranes are the technical problems associated with wear of the wheels and the crane track, which causes crane skewing. The main causes of crane skewing include unevenness of the crane track, unequal loading of the traction drives depending on the position of the crane trolley, slips and different sizes of travel wheels and combinations of these causes. Firstly, this paper presents a design solution that can be used to detect the magnitude of mechanical stress and deformation of the steel structure of the crane, caused by the effects of skewing. The mechanical stress generated by the transverse forces of the deformed geometric shape of the crane bridge structure is recorded by mechanical stress detectors installed in the inner corners of the crane bridge. The resulting electrical signal from element mechanical voltage detectors, loaded by axial forces, can be used for feedback control of separate crane travel drives controlled by frequency converters. Secondly, this paper presents the calculation of the lateral transverse forces according to CSN 27 0103 and the determination of the values of mechanical stresses of the deformed steel structure of the crane bridge of a two-girder bridge crane using the finite element method in the program MSC.MARC 2019. Finally, this paper presents the structural and strength design of mechanical stress detectors and the conclusions of laboratory tests of axial force loading of mechanical stress detectors on the test equipment. At the same time, it presents records of the measured axial forces acting in the mechanical stress detectors, arising from the deformation and warping of the crane bridge by the known magnitude of the axial force acting on the crossbeam and from the deformation of the crane bridge caused by the crane operating modes.

Elimination of crane skewing on crane tracks is currently based on several principles, of which the best known and most widely applied in practice are the optical methods [1], ultrasonic [2] and strain gauges [3,4]. The “Geotronics” [5] optical method is based on the principle of evaluating the speed of movement of laser beams. Laser transmitters are placed on both end faces of the crossbeams in the direction of travel of the crane, and reflector elements of the laser beams are located at the end points of the crane tracks. During continuous measuring of the distance of the laser transmitters from the reflectors, signals are sent to the drive to control the speed of the driving electric motors. The principle of “Electronic flanges” [2] uses four ultrasonic sensors, which continuously measure the lateral distance of the corner parts of the crane bridge from the railhead. The control circuit (programmable logic controller) evaluates four sensor signals. The output signal from the controller enables independent control (by changing the travel speeds of the right and left side of the crane controlled by frequency converters) of the circumferential speeds of the driving crane wheels.

The principles [1,2] are based on the assumption that travel wheels with double-sided flanges mounted on opposite crossbeams (driven by separate drives) run parallel, and thus travel the same path in the same moment of time. This principle is also used by mechanisms with a fixed or electric shaft, which can achieve the same speed of the drive motors, but due to different gears it is not possible to ensure uniform wear of the wheels, resulting in increased stress on the steel structure of the crane from the even travel of opposing sides (crossbeams) of the truck.

In industrial practice, it is possible to eliminate or completely negate the effects of crane skewing on bridge-type cranes by a method that is based on the control of traction motors [5] with regard to minimizing the mechanical stress of the crane structure

* Corresponding author.
E-mail address: leopold.hrabovsky@vsb.cz (L. Hrabovský).

https://doi.org/10.1016/j.taml.2021.100299

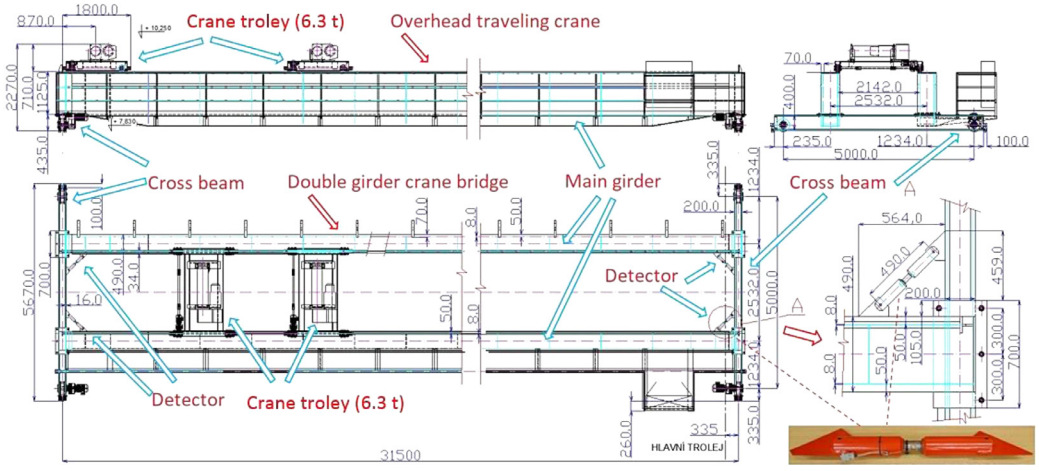

Fig. 1. Double-girder overhead crane 2 × 6.3 t-31.5 m.

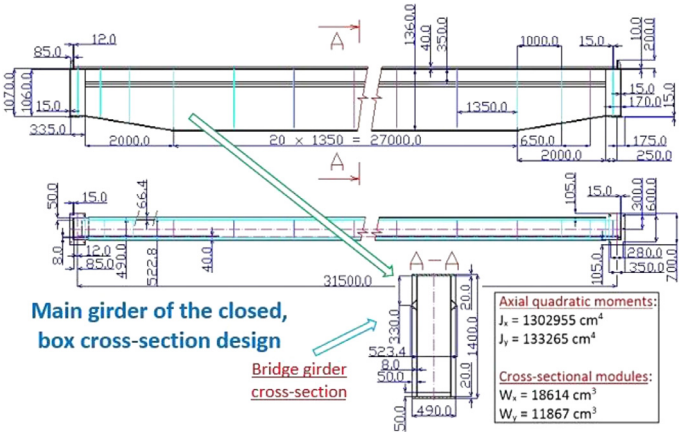

Fig. 2. Main girder of two-girder bridge crane 2 × 6.3 t-31.5 m.

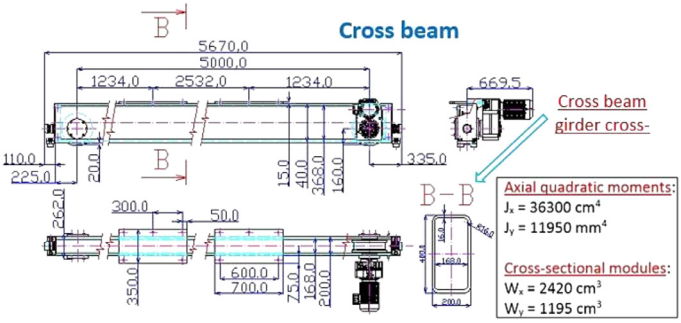

Fig. 3. Cross beam of the two-girder bridge crane 2 × 6.3 t-31.5 m.

[3,4]. In this method, information on deformation and mechanical stress is obtained from strain gauge bridge sensors [6,7] located at a suitable place on the crane bridge structure. The magnitude of the deformation of the steel structure of the crane bridge often does not reach such optimal magnitudes that would make it suitably detectable by foil strain gauges attached to selected places of the crane bridge [4].

More suitable solution for gaining knowledge on the magnitude of mechanical stress in the deformed structure of a crane bridge is to install so-called mechanical stress detectors (hereinafter MSD) in pre-selected places on the crane bridge [8]. The MSDs are usually mechanically attached in places of the steel structure of the crane bridge [9], where the ends of the main girders are connected to the crossbeams, see Fig. 1.

The effects of transverse loads, which according to CSN EN 13001-2 + A3 [10] are included in the category of intermittent loads, when the crane travels along a crane track formed by steel rails, were detected on a double girder bridge crane 2 × 6.3 t-31.5 m, see Fig. 1.

The main girder of the crane and its static cross-sectional values are shown in Fig. 2.

The cross beam of the crane and its static cross-section values are shown in Fig. 3.

According to CSN 27 0103 [11], the horizontal lateral forces H_{tpv}, from the crane skewing on the crane track can be determined according to relation (5). The crane skewing factor λ in Eq. (1) assumes the following limit values: $0.05 \leq \lambda \leq 0.2$. K_1 (Eq. (3)) K_2

Table 1
Base parameters of a two-girder bridge crane.

Crane load capacity m_q (kg)	2 × 6300
Total crane weight m_c (kg)	29676.2
Crane block weight m_k (kg)	1095.4
Crane gauge (Runway length) L (mm)	31500
Crane wheelbase s (mm)	5000
Block travel distance L_1 (mm)	870
Block length L_2 (mm)	1800

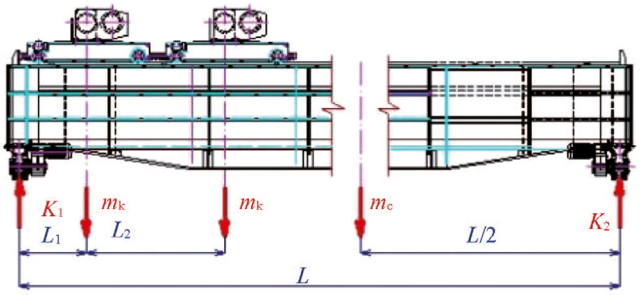

Fig. 4. Calculation diagram for calculation of wheel loads K_1 (N) and K_2 (N) according to CSN 27 0103.

(Eq. (2)), the wheel load on the more (less) loaded branch of the crane track from the net weight of the crane m_c (see Table 1) and the block m_k with a total load m_q is in the most efficient position (Fig. 4).

$$\lambda = 0.025 \times \frac{L}{s} = 0.025 \times \frac{31.5}{5.0} = 0.158, \quad (1)$$

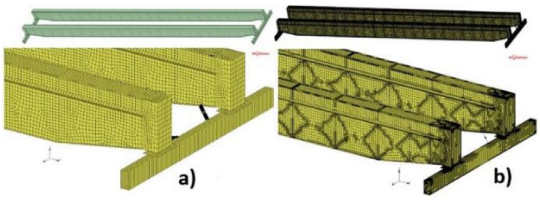

Fig. 5. Finite element method (**a**) starting, (**b**) resulting finite element network.

$$K_2 = \frac{(m_2 - 2m_k) \times g \times \frac{L}{2}}{L} + \frac{(m_k + 2m_q) \times g \times L_1 + (m_k + 2m_q) \times g \times (L_1 + L_2)}{L} = 144.92 \text{ kN} \quad (2)$$

$$K_1 = \frac{(m_c - 2m_k) \cdot g \cdot \frac{L}{2}}{L} + \frac{(m_k + m_q) \cdot g \cdot (L - L_1) + (m_k + m_q) \cdot g \cdot (L - L_1 - L_2)}{L} = 269.66 \text{ kN} \quad (3)$$

$$H_{tp} = \lambda \times K_1 = 0.158 \times 269.66 \times 10^3 = 41.47 \text{ kN}, \quad (4)$$

$$H_{tpv} = H_{tp} \times \gamma_{tp} = 42.47 \times 10^3 \times 1.1 = 46.72 \text{ kN}, \quad (5)$$

$$P_y = H_{tpv} \times \frac{s}{L} = 46.72 \times 10^3 \times \frac{5}{31.5} = 7.42 \text{ kN}. \quad (6)$$

The final value of axial force $P_{yc} = 8$ kN is selected by rounding.

Calculation of applied mechanical stresses and axial forces in the measuring element MSDs and deformation of the steel structure of crane bridge of double girder bridge crane 2 × 6.3 t-31.5 m (Fig. 1) was performed by finite element method (FEM) in the MSC.MARC 2019 program. During the calculation, the geometric model of the crane was transformed into a shell (this is suitable for thin-walled structures, which the box-type beams (Fig. 2) and even crossbeams (Fig. 3) of the 2 × 6.3 t-31.5 m crane can be considered), which allows using fewer elements in the FEM calculation and thus greatly shortens the computation time.

A "relatively coarse" network was used to calculate the FEM, see Fig. 5a, formed by isoperimetric square shell elements with a maximum size of 50 mm. An adaptive networking technique was used to refine the network, Fig. 5b. This is a process where, according to a certain criterion, the size of the elements is reduced locally to increase the accuracy.

At the maximum axial force P_{yc} Eq. (5), the axial force of the maximum value $F_{med(1)}$ = -43.3 kN (see Table 2), which was determined by FEM, arises at the measuring element "1" (see Fig. 6c) MSD. The minimum value of the cross section S_{min} of the measuring element MSD can be determined according to relation Eq. (7).

$$R_{ev} = \frac{F_{med(1)}}{S_{min}} \Rightarrow S_{min} = \frac{F_{med(1)}}{R_{ev}} = \frac{43.3 \times 10^3}{137.5 \times 10^6} = 3.15 \text{ cm}^2. \quad (7)$$

In the FEM calculation, one of the girders (left girder on Fig. 1) is assigned these boundary conditions (see Fig. 6a): at the placement location of the driven crane wheel, travel in the direction of crane travel (z-axis) and travel in the y-axis are prevented (travel shifts u, v, w see Fig. 6a represent travel along the respective x, y, z axes). The force pair H_{tpv} in Eq. (5) is introduced into the pins of crane wheels mounted on the opposite crossbeam (right in Fig. 6a). In the FEM computational model, the crane blocks are represented by material points connected with an assembly of MPC bonds. The blocks are fully loaded with the weight of the load, meaning that at both material points a force is exerted that is equivalent to the maximum load capacity of the blocks $m_q = 6.3 \times 10^3$ kg.

During the calculation, 3 stress cases were considered, which were applied sequentially: gravitational force load, load by burden and load by a force pair H_{tpv} in Eq. (5). A continuous network was used for the calculation, and in places where it was not possible to connect the elements by means of a network (places where gaps between the elements were created due to the use of shells), "glue" type contacts are used.

The purpose of the FEM calculation in the MSC.MARC 2019 software environment was to determine the magnitude of the mechanical stress $\sigma_{med(i)}$ in the MSD measuring elements (2, Fig. 7), which are located in the corner parts of the crane bridge (Fig. 1), meaning in places where the lower flanges of the main girders (Fig. 2) are connected to the crossbeams (Fig. 3). In the MSD measuring elements, the highest normal stress $\sigma_{med(i)}$ in the central surfaces of the shells was evaluated, meaning in the center parts of the cross-sectional thickness S_s of the MSD measuring elements. In Fig. 6c, the measuring MSD measuring elements are indicated by numbers 1 to 4 and the crane blocks are shown schematically. From the FEM results obtained, it is possible to calculate the resulting axial forces, $F_{med(i)}$ (see Table 2), acting in the measuring elements of the MSD. Figure 6b shows the course of the largest normal voltage $\sigma_{max(1)}$ in the measuring element MSD "1" with a cross section S_s Eq. (8).

$$S_s = \frac{\pi \times \left(D^2 - d^2\right)}{4} = \frac{\pi \times \left(0.03^2 - 0.022^2\right)}{4} = 3.27 \text{ cm}^2. \quad (8)$$

In the MSC.MARC 2019 software environment, the FEM determined the mean value of the "median" stress $\sigma_{med(i)}$ and the normal forces $F_{med(i)}$ (inducing the stress $\sigma_{med(i)}$ on the cross-sectional area S_s in Eq. (8) of the shell) in the individual MSD measuring elements, see Table 2.

The mechanical stress according to the HMH hypothesis was determined in all components of the crane bridge and was checked in the outer and inner layers of the shells. The stress in certain components (e.g. sidewalls) was affected by the occurrence of singularities (places where there is an unrealistic increase in stress as the size of the element decreases). Singularities occur at sharp corners at the joints of sheet metal parts and are only of a local nature. Since the area of interest was to determine the stresses in the measuring elements of the MSD, the stresses in the other components were determined at sufficient distances from these singularities. The course of mechanical stress in the steel structure of the crane bridge is shown in Fig. 8a (on the side of detail A there are blocks which are not shown in Fig. 8a). The singularities in the sidewalls (see detail B) are shown in Fig. 8b, and the voltage outside the singularity is shown in Fig. 8c.

The material 11523.1, from which the measuring element (2, Fig. 7) ϕ 30/22 mm MSD is made, acquires a yield strength R_e = 275 MPa. It is assumed that the measuring elements 2 (glued with foil strain gauges 1-XY11-6/350 [12, pp. 28/96]) will be loaded to a maximum of 50% of the yield strength R_e, meaning $R_{ev} = 0.5R_e$ = 137.5 MPa.

The main part of the MSD is the so-called measuring element (2, Fig. 7) whose cross section S_s (8) and construction dimensions are designed so that it senses the mechanical stress σ_m acting on

Table 2
Detected values of the relative U_m of the MSD loaded by the force F_T of the hydraulic jack.

MSD	FEM		C2 Sensor		Measuring element of sensor		
i(-)	$\sigma_{med(i)}$(MPa)	$F_{med(i)} = \sigma_{med(i)} \cdot S_s$(kN)	$U_{c(i)}$(mV/V)	$F_{T(i)}$(kN)	$U_{m(i)}$(mV/V)	$\sigma_{m(i)}$(MPa)	$k_{m(i)} = F_{T(i)}/U_{m(i)}$(kN/mV/V)
TA	-	-	1.04 (10)	26.00*1	0.288*1	45.17 (11)	90.28
	132.4	43.3	1.07	26.75	0.296	46.42	90.37
			1.03	25.75	0.282*2	44.23	91.31
NB	97.4	31.8	1.11	27.75	0.235	36.86	118.09
			1.10	27.50	0.234	36.70	117.52
			1.03	25.75	0.225*2	35.29	114.44
TC	-	-	1.04	26.00	0.266	41.72	97.74
	62.7	20.5	0.995	24.88	0.296	46.42	84.05
			1.03	25.75	0.282*2	44.23	91.31
ND	40.5	13.2	1.14	28.50	0.312	48.93	91.35
			1.16	29.00	0.309	48.46	93.85
			1.06	26.50*3	0.275*2,3	43.13	96.36

*1 see Fig. 10.
*2 see Eq. (12).
*3 see Fig. 13.

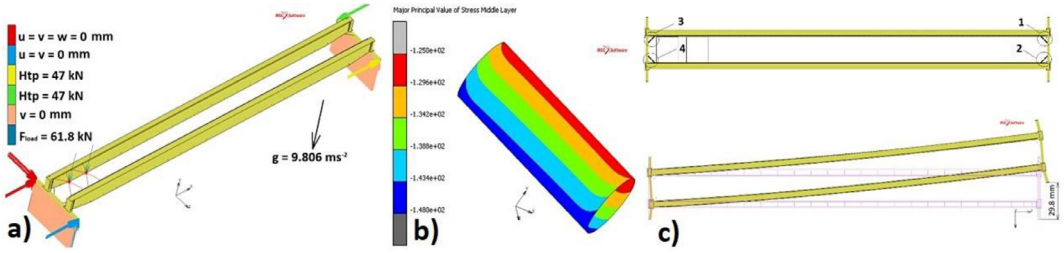

Fig. 6. (**a**) The boundary conditions of the FEM calculation, (**b**) course of the normal stress in the measurement area by MSD, (**c**) deformation of the crane bridge.

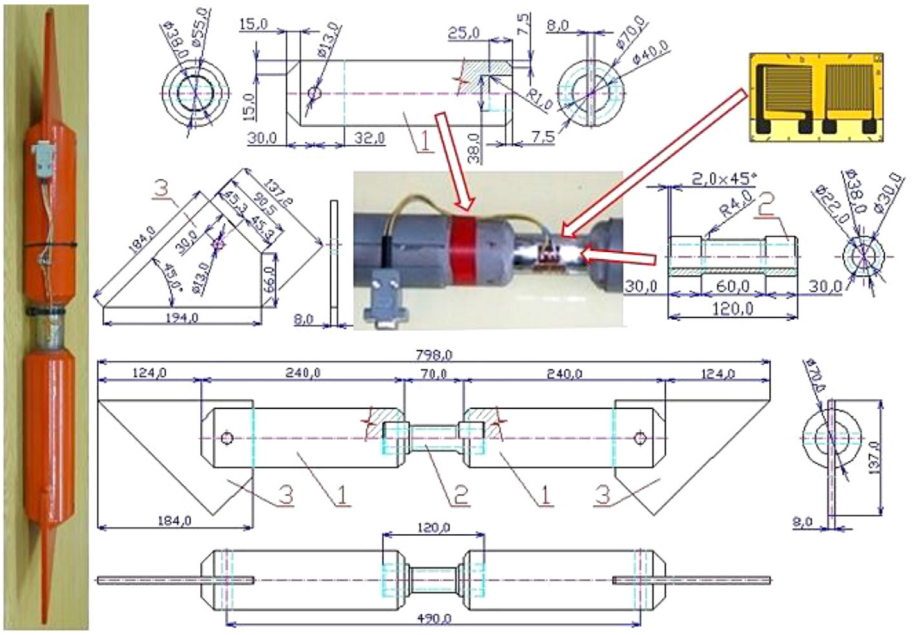

Fig. 7. Dimensional parameters of MSD component parts.

it over the whole range of its limit values. Measuring element 2 MSD, see Fig. 7, with an actual cross section S_s (8), is designed as a tube with an outer diameter $D = 30$ mm and an inner diameter $d = 22$ mm.

With the force pair H_{tpv} (5) acting on the steel structure of the crane bridge 2 × 6.3 t-31.5 m (Fig. 6a), a mechanical stress, $\sigma_{max} = 132.4$ MPa, is generated in the cross section S_s (8) of the MSD measuring element (see Fig. 6b). The maximum axial force F by which the MSD measuring element (2, Fig. 7) installed on the bridge crane 2 × 6.3 t-31.5 m can be loaded, can be determined according to relation Eq. (9). Figure 6c shows the deformation of the crane bridge structure and the mean amount of movement of the crossbeam $D_z = 29.8$ mm, when the force pair H_{tpv} (5) acts on the crane bridge 2 × 6.3 t-31.5 m according to CSN 27 0103 [11].

$$F = \sigma_{max} \times S_s = 132.4 \times 10^6 \times 3.27 \times 10^{-4} = 42.3 \text{ kN}. \quad (9)$$

For the purposes of MSD calibration, the Yokogawa DL750 [13] measuring apparatus was used, in which relation (11) [7, p.13] is used for the calculation of the measured stress value σ_m of the

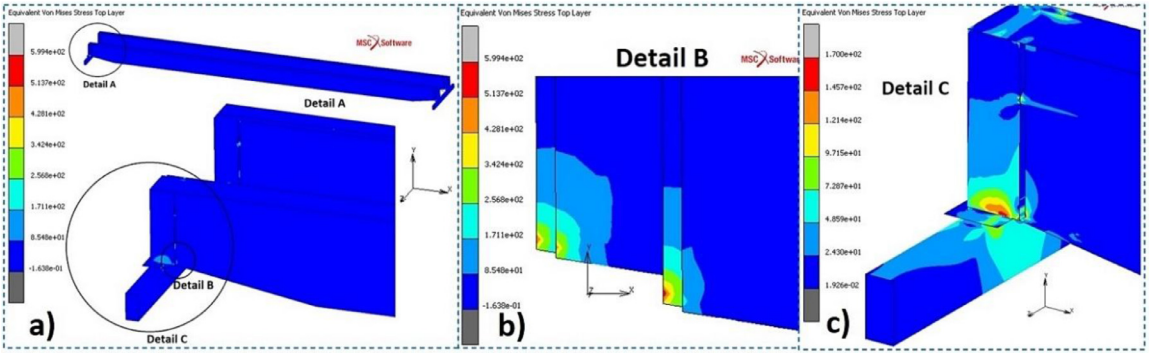

Fig. 8. (**a**) Course of the stress according to HMH in the structure, (**b**) occurrence of singularities in sidewalls, stress according to HMH, (**c**) stress according to HMH in sheets outside singularities.

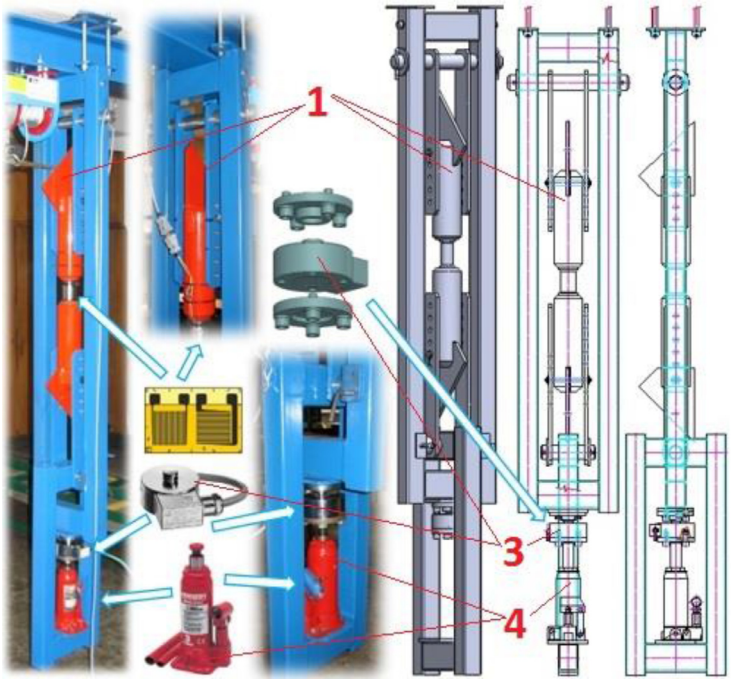

Fig. 9. MSD testing device.

deformed cross section S_s of the MSD measuring element covered with resistance film stress gauges (1-XY11-6/350 [12]).

Assuming that at the maximum possible load of the tensile force transducer 5×10^3 kg $\cong$ 50 kN it is possible to read the voltage value $U = 1$ V at 1000 times gain at the supply voltage $U_N = 5$ V of the pressure force transducer C2 [14], then the voltage $U_c = 1.04$ mV/V corresponds to the tensile force F in Eq. (10), see Table 2.

$$\frac{c_{nom}\text{mV/V}...50\text{kN}}{U_c\text{mV/V}...F_T\text{kN}} \Rightarrow F_T \times 50 = U_c \times c_{nom}$$
$$\Rightarrow F_T = \frac{U_c \times 50}{c_{nom}} = \frac{1.04 \times 50}{2} = 26 \text{ kN}. \quad (10)$$

To verify the functional properties of the MSD (Fig. 7) on the test equipment (Fig. 9), the MSD 1 were subjected to a tensile force F_T exerted by the compressive force of the hydraulic jack 4, the instantaneous value of which was detected by the tensile force sensor C2 3. On the display of the Yokogawa DL750 [13] measuring apparatus, it was possible to read the instantaneous value of the compressive force F_T derived by the hydraulic jack 4, which manifests itself as a tensile force on the MSD measuring element 1. At the same time, the time course of the proportional extension U_m of the MSD measuring element is shown on the display of the measuring apparatus [13], see Table 2.

$$s_m = \frac{4 \cdot U_m \times E}{k \times n_t \cdot 10^3} = \frac{4 \times 0.288 \times 2.1 \times 10^{11}}{2.06 \times 2.6 \times 10^3} = 45.17 \text{ MPa}, \quad (11)$$

where $n_t = 2.6$ for the total number of strain gauges used 4 (of which 2 strain gauges are glued longitudinally and measure longitudinal elongation and 2 strain gauges are glued transversely and measure transverse contraction, $n_t = 2 + 2\mu = 2.6$, pro $\mu = 0.3$).

On the display of the Yokogawa DL750 measuring apparatus, it was possible to read the instantaneous value of the compressive force F_T (Fig. 10) derived by the hydraulic jack 4 (see Fig. 7) which manifests itself as a tensile force on the MSD measuring element 1.

The 2 × 6.3 t-31.5 m bridge crane (Fig. 1) without load (i.e. without suspended load of mass m_q on the hook of both crane blocks), with crane blocks located in the middle of the span of the crane bridge, was moved several times manually and backwards and forward, with released travel brakes, in the direction of the

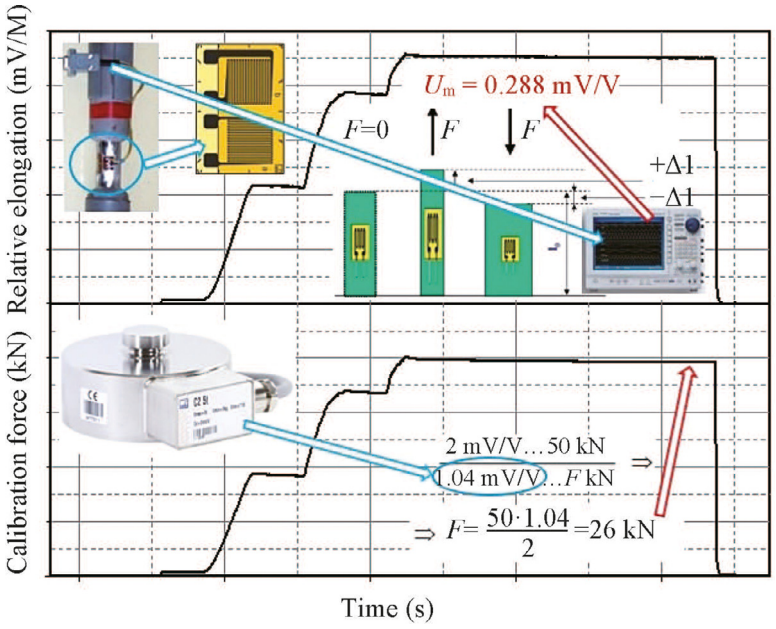

Fig. 10. Record of relative during experimental test of the MSD Yokogawa DL750 measuring apparatus.

crane track in order to release the internal stress in the steel structure of the crane in the horizontal direction.

After the crane movement was completed, it was checked whether all wheel flanges of the wheels are equally spaced from the sides of the railheads (wheel diameter $D_k = 320$ mm, distance between wheels $a = 75$ mm, rail width $b = 55$ mm). After verifying the identical distance of the flanges from the sides of the railheads, four MSDs (Fig. 7) (which were marked TA, NB, TC and ND) were welded in the inner corners of the crane bridge, see Fig. 15.

The solder pads of each 1-XY11-6/350 strain gauge [12] (glued to the measuring section, see 2 Fig. 7, MSD) were conductively connected with a 3-core cable to the corresponding connectors of the 9-pin D-SUB socket. Each of the four MSDs was connected via its own electrical cable (terminated with a 9-pin D-SUB plug) to a Yokogawa 750 [14] measuring apparatus.

A bracket P (Fig. 11) was welded to the vertical steel girder at the end of the crane track so that the longitudinal axis of the hub 8 was concentric with the axis of the bumper attached to the front face of the crossbeam (Fig. 3) of the crane bridge. A hydraulic jack 4 [15], hubs 5 and 6, mechanically connected using screws, and a strain gauge load cell 3 [15] were placed on the bracket (see $\underline{P}$, Fig. 11), to which a hub 8 was attached by screws, the front surface of which rested on the spring bumper of the crane (Fig. 11) (which was secured against compression).

The travel wheels of the crane bridge placed in the second crossbeam (on the opposite side of the crane bridge) were secured with a stop (mechanically attached to the crane rail) against overrunning (i.e., shifting in the direction of the crane travel). After locking the travel wheels of the opposite crossbeam and completing the installation of the bracket (P, Fig. 11), a horizontal force $P_{yc} = 8$ kN in Eq. (6) was exerted by the hydraulic jack $\underline{4}$ onto the front surface of the crossbeam, in the direction of crane travel.

The horizontal force P_{yc} and the values of the relative $U_{m(i)}$ of the DMS component measuring elements were detected by the strain gauge C2, see Fig. 12a, and these signals were recorded by a Yokogawa 750 [13] measuring apparatus. Figure 12b and Table 3 present the values of the axial forces $F_{m(i)}$, which can be calculated according to relationship Eq. (12) if the values of the relative $U_{m(i)}$ (mV/V) of the respective MSD are known (they are read by the measuring apparatus Yokogawa 750).

$$F_{m(i)} = U_{m(i)} \times k_{m(i)}(\mathrm{N}), \tag{12}$$

After connecting all eight strain gauges T1 (T5), T2 (T6), T3 (T7) and T4 (T8), see Fig. 15, placed on the SMD, into the Wheatstone resistor bridge and supplying the electrical signal U_{mc} (mV/V) in Eq. (13), which is given by the "sum of signals (TA - NB + TC - ND)/2" (see Table 3) from the MSD, graphic records were obtained into the measuring apparatus Yokogawa 750 [13], see Fig. 13.

$$\begin{aligned} U_{mc} &= \frac{k}{4} \times (U_{mTA} + U_{mNB} + U_{mTC} + U_{mND}) \\ &= \frac{2.06}{4} \times (0.152 + 0.149 + 0.108 + +0.145) \\ &= \frac{2.06 \times 0.554}{4} = 0.285 \text{ mV/V}. \end{aligned} \tag{13}$$

After removing the stop, which prevented the travel (in the direction of travel of the crane) of the travel wheels placed in the second crossbar, i.e. after releasing the crane on the previously braked side and removing the bracket $\underline{P}$ (Fig. 11), the 2 × 6.3 t-31.5 m crane was ready for operational measurements.

Operational measurements recorded the generated forces, which are manifested during the working cycle of a two-girder bridge crane. The effects of crane bridge deformation were detected for: 1) travel of unloaded (Fig. 14) and loaded crane with blocks in the middle of the bridge, 2) travel of unloaded and loaded crane with blocks moved to the extreme edge of the bridge, 3) suspension and lifting of loads with blocks in the center, as well as moved to the edge of the bridge and 4) lowering the load with blocks in the middle, and moved to the edge, of the bridge.

The 2 × 6.3 t-31.5 m bridge crane (Fig. 1) without load, with crane blocks located in the middle of the crane bridge span, was driven along the length of the crane track and the induced internal stress in the steel structure of the crane bridge was detected by installed MSDs. Instantaneous values of axial forces, see Fig. 14, acting on the individual measuring elements of the MSD from the effects of the crane skewing were recorded by the Yokogawa 750 [13] measuring apparatus.

All eight strain gauges T1 (T5), T2 (T6), T3 (T7) and T4 (T8) are connected to a Wheatstone resistance bridge, see Fig. 15. The out-

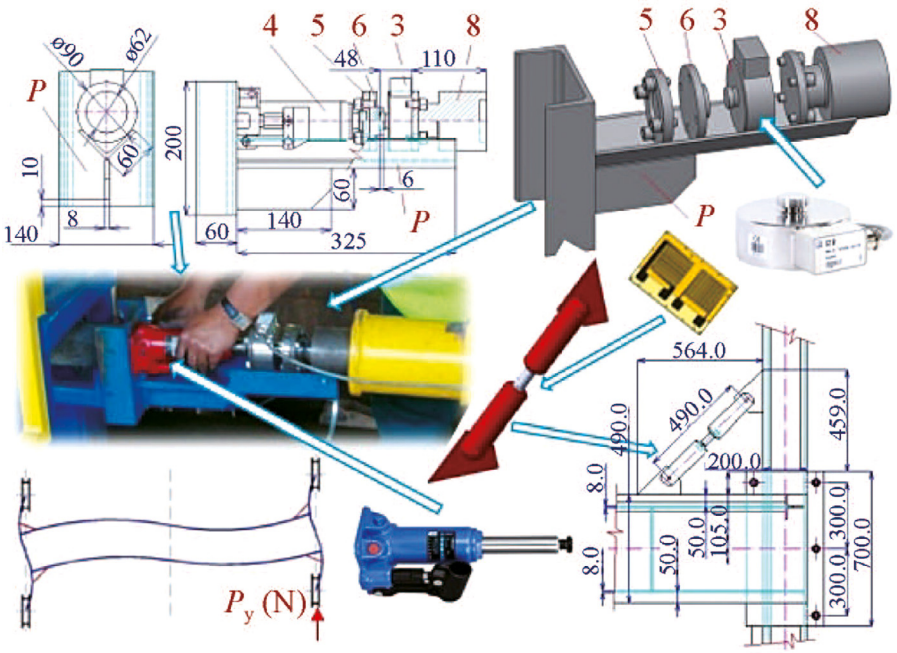

Fig. 11. Platform $\underline{P}$ supporting the array of machine parts used exerting and detecting compressing force P_{yc}.

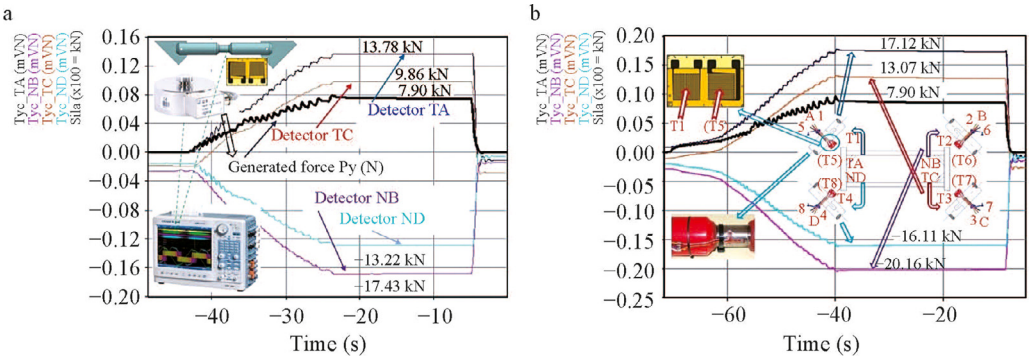

Fig. 12. Record of relative during experimental test of the MSD Yokogawa DL750 measuring apparatus.

Table 3
Detected values of a relative $U_{m(i)}$ of the MSD during skewing of the crane bridge by axial force P_{yc}.

MSD	C2 Sensor			Measuring element of sensor		
i(-)	$U_{c(i)}$(mV/V)	$k_{c(i)} = F_{c(i)}/U_{c(i)}$(kN/mV/V)	$F_{c(i)}$(kN)	$U_{m(i)}$(mV/V)	$k_{m(i)} = F_{T(i)}/U_{m(i)}$(kN/mV/V)	$F_{m(i)}$(kN)
TA	0.316	25	7.90	0.152	(90.28 + 90.37 + 91.31) / 3 = 90.65	13.78*1
				0.189		17.12*2
NB				- 0.149	(118.09 + 117.52 + 114.44) / 3 = 116.68	- 17.43
				- 0.173		- 20.16
TC				0.108	(97.74 + 84.05 + 91.31) / 3 = 91.03	9.86
				0.144		13.07
ND				- 0.145	(91.35 + 93.85 + 96.36) / 3 = 93.85	- 13.22
				- 1.177		- 16.11

*1 Fig. 12a.
*2 Fig. 12b.

put signal from the measuring bridge is fed via a single-channel measuring amplifier (Industrial Amplifier) from Hottinger Baldwin Messtechnik GmbH under the trade name CLIP AE301 [16] to the Yokogawa 750 [13] measuring apparatus.

A record of the entire range of experimental measurements performed of the relative deformations of partial MSDs caused by the crane travel and the suspension of the load is presented (see Fig. 6a). The sum signal U_{mc} of the relative deformations of the four MSDs is presented in Fig. 6b.

The highest value of proportional deformation in the MSD measured in the record shown in Fig. 16a corresponds to 0.12 mV/V, which, in comparison with the voltage U_m = 0.312 mV/V (see Table 2), which corresponds to the standard CSN 270103, where P_{yc} = 8 kN and H_{tp} = 47 kN, corresponds to 38% of the calculated

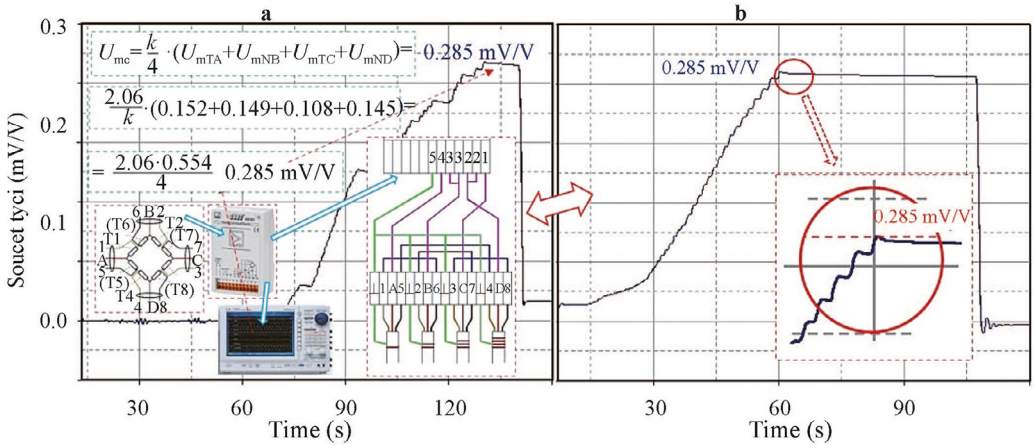

Fig. 13. Sum signal U_{mc} in Eq. (12) of the component axial forces detected by the MSD (see Fig. 12) from the deformation of the crane bridge.

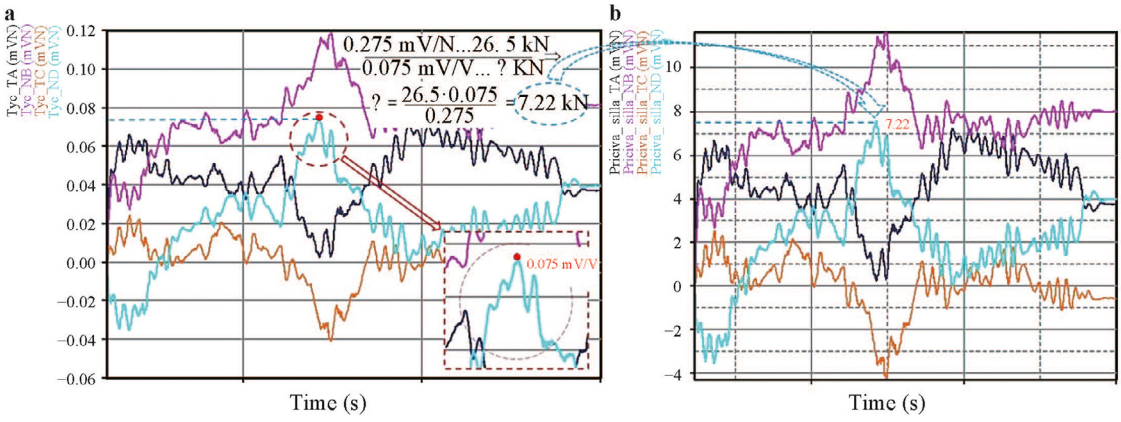

Fig. 14. Course of (**a**) relative, (**b**) axial forces in the MSD from the effect of crane bridge deformation during crane travel.

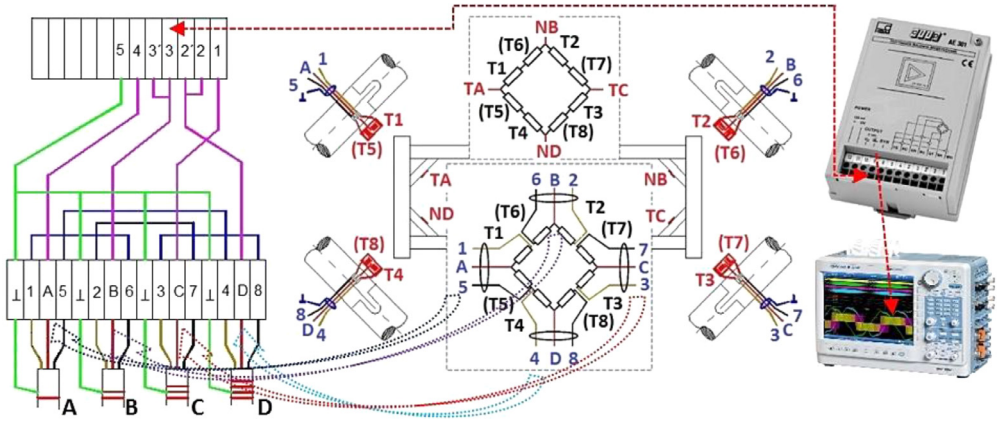

Fig. 15. Electrical connection of strain gauges from MSD to Wheatstone resistor bridge in the CLIP AE301 amplifier.

transverse force (H_{tpv} = 47 kN in Eq. (5) or Fig. 6a) according to the CSN 270103 standard.

The sum signal U_{mc} of the relative deformations of the four MSDs, see Fig. 16b, can be used for feedback control of separate crane travel drives controlled by frequency converters.

The aim of the operational measurements performed on the 2 × 6.3 t-31.5 m crane was to obtain an electrical signal with properties that will allow to control the frequency converters regulating the speed of the traction motors, which can eliminate the effects of crane skewing to a minimum.

To obtain the values of mechanical stress in the required places of deformation and known size (standard CSN 27 0103 recommended) force pair H_{tpv}, steel structure of the crane, a 3D geometric model of the crane bridge was created. In the MSC.MARC 2019 program, the finite element method (FEM) was used to calculate the normal stress in the measuring elements of mechanical stress detectors (hereinafter only MSD), mechanically mounted in the inner corner parts of a two-girder crane bridge.

From the calculation of the maximum value of normal stress $\sigma_{med(TA)}$ = 132.4 MPa obtained in the measuring element MSD "TA", the actual cross section S_s = 3.27 cm^2 of all four measuring elements MSD was determined, which were glued with resistance foil strain gauges after their production.

In the laboratory, all four MSDs were gradually subjected to a tensile force of $F_T \cong$ 26 kN on a test rig, the magnitude of which was generated by a hydraulic jack and detected by a strain gauge

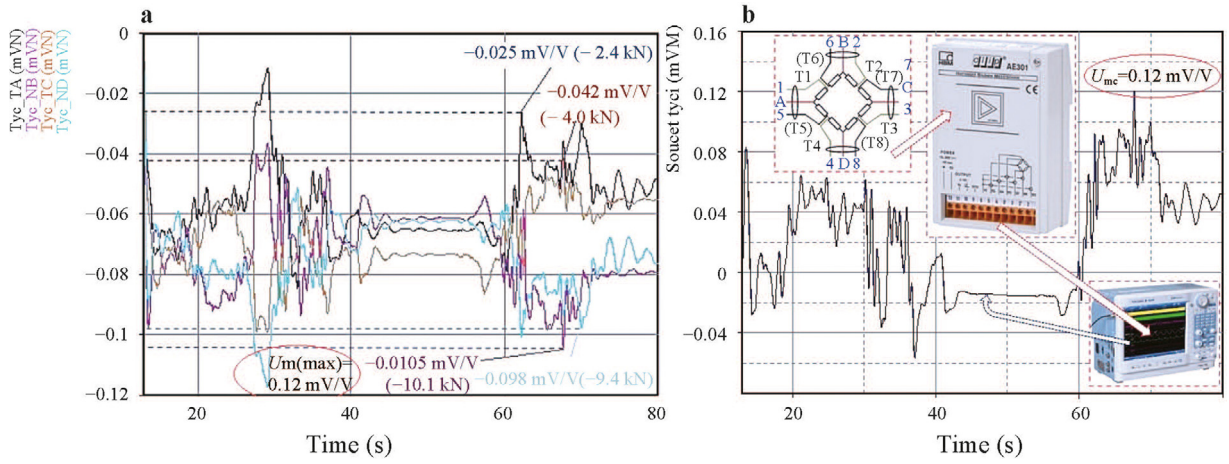

Fig. 16. Course of (**a**) partial relative elongations, (**b**) total relative elongation of the MSD from the effect of crane bridge deformation caused by crane travel and load suspension.

load cell. With a known magnitude of the acting tensile force F_T, a constant k_m was determined for each MSD. If the measured elongation signal of the respective MSD $U_{m(i)}$ (mV/V), obtained from the measuring apparatus Yokogawa 750, is multiplied by the constant $k_{m(i)}$, this result of the multiplication can be used to define the mechanical stress $\sigma_{m(i)}$ acting in the i-th MSD measuring element.

The partial MSDs were connected to the inner corners of the crane bridge by welded joints and then two types of test trials were performed on a double girder bridge crane.

The purpose of the first test trial was to obtain the values of the actual mechanical stresses acting in the MSD measuring elements with the exertion of the axial force P_{yc} into the front face of one of the crane crossbeams, provided that the other crossbeam is prevented from moving in the crane's travel direction. The axial force P_{yc} = 8 kN exerted by a hydraulic jack, when moving the front surface of the crossbeam in the direction of crane travel with the value D_z = 30 mm, excites the highest value of compressive force $F_{m(NB)}$ = 20.16 kN in the measuring element MSD "NB" (see Table 3 and Fig. 6), which corresponds to a stress of $\sigma_{m(NB)}$ = 61.65 MPa at the cross section S_s of the MSD measuring element. The obtained maximum value of mechanical stress acting in the MSD measuring element from the experiment ($\sigma_{m(NB)}$ = 61.65 MPa) is, compared with the value of stress determined by the calculation of FEM ($\sigma_{med(TA)}$ = 131.4 MPa, see Table 2), about 47%.

The detected values of the relative $U_{m(i)}$ of the individual MSDs during the deformation of the crane bridge by the axial force P_{yc} were connected in the required order to the Wheatstone resistance bridge in the single-channel measuring amplifier CLIP AE301. The output sum signal U_{mc} of the proportional deformations of the four MSDs can be used for the feedback control of the separate crane travel drives controlled by frequency converters.

The purpose of the second test was to obtain the values of the actual mechanical stresses that are generated in the measuring elements of the MSD during the warping of the crane bridge from the force effects that are manifested in the individual modes of the crane work cycle.

The maximum value of the relative of the MSD from the effect of crane bridge warping caused by crane travel and load suspension was measured as $U_{m(ND)}$ = -0.12 mV/V (see Fig. 16a), which in comparison with the voltage U_m = 0.312 mV/V (see Table 2) corresponds to 38% of the calculated transverse force H_{tpv}. The sum signal U_{mc} of the proportional deformations of the four MSDs (see Fig. 16b) can also be used for the feedback control of the separate crane travel drives controlled by frequency converters.

The solution described in this article is based on there being places on the supporting structure of the crane where the proportional deformations from transverse forces and from eccentric braking are the highest in terms of values. Therefore, at these sites, MSDs are placed, and fitted with strain gauge sensors of proportional deformations, where the highest proportional deformations are caused by transverse or eccentric braking. The individual strain gauges are connected to a special chain in the Wheatstone resistance bridge so that the measured values of proportional deformations from skewing or transverse or eccentric braking add up and other loads, especially symmetrical loads, to be canceled out, which the special strain gauge chain reliably performs. This provides a distinctive electrical impulse signaling the start of skewing or eccentric braking, which serves as information for the feedback control of the separate drives of the crane trucks controlled by frequency converters. By slightly changing the speed of one side of the truck compared to the other side of the truck, which is determined by the signals from the strain gauge in terms of polarity and magnitude, the lateral and eccentric braking can be reduced to a minimum.

This work has been supported by The Ministry of Education, Youth and Sports of the Czech Republic from the Specific Research Project SP2021/53.

Declaration of Competing Interest

Manuscripts by name "Detection of Mechanical Stress in the Steel Structure of a Bridge Crane, was not been previously published in any language anywhere and that it is not under simultaneous consideration or in press by another journal.

References

[1] D. Aust, J. Tomis, Eliminace příčení mostových a portálových jeřábů, MM Průmyslové spektrum 9 (2006) www.mmspektrum.com/vydani/2006/9/1. (In Czech).
[2] Emotron - jeřábové pohony s frekvenčními měniči, from https://www.elprodrive.cz/cz/produkty/pohony-jerabu.php, accessed on 2021-06-17. (In Czech)
[3] A. Zelic, N. Zuber, R.A. Sostakov, Experimental determination of lateral forces caused by bridge crane skewing during travelling, Eksploatacja i Niezawodnosc 20 (2018) 90–99, doi:10.17531/ein.2018.1.12.
[4] J. Kulka, M. Mantic, G. Fedorko, et al., Failure analysis concerning causes of wear for bridge crane rails and wheels, Eng. Failure Anal. 110 (2020) 1–14, doi:10.1016/j.engfailanal.2020.104441.
[5] N. Mitrovic, V. Kostic, M. Petronijevic, et al., Multi-motor drives for crane application, Adv. Electr. Comput. Eng. 9 (2009) 57–62, doi:10.4316/AECE.2009.03011.
[6] L. Hrabovsky, Z. Folta, Detectors of mechanical stress limiting effects of crane structure deformation (2021). (In the press)

[7] Z. Folta, Odporová Tensometrie. (2015). https://slideplayer.cz/slide/12090281/. (In Czech)
[8] L. Hrabovsky, Action on crane runway caused by horizontal forces due to crane skewing, Key Eng. Mater. 669 (2016) 391–399, doi:10.4028/www.scientific.net/KEM.669.391.
[9] Snížení příčení pojezdu jeřábů, from https://www.temex.cz/specializace/rizeni-jerabu/snizeni-priceni-pojezdu-jerabu/, accessed on 2021-03-21. (In Czech)
[10] ČSN EN 13001-2+A3 Crane safety - General design - Part 2: Load actions. (In Czech: Jeřáby - Návrh všeobecně -Část 2: Účinky zatížení). TNK 123, Zdvihací a manipulační zařízení, Praha.
[11] ČSN 27 0103 Design of steel crane structures. (In Czech: Navrhování ocelových konstrukcí jeřábů. Výpočet podle mezních stavů). TNK 123, Zdvihací a manipulační zařízení, Praha.
[12] HBM strain gauges, from www.hbm.cz/wp-content/uploads/S01265.pdf, accessed on 2021-06-14.
[13] DL750/DL750P ScopeCorder, from https://tmi.yokogawa.com/solutions/discontinued/dl750dl750p-scopecorder/, accessed on 2019-11-01.
[14] C2 Force Transducer, www.hbm.cz/wp-content/uploads/B00656.pdf, accessed on 2021-05-25.
[15] Vozový zvedák hydraulický 3 tuny, from www.naradiprofesional.cz/207594-workersbest-t90304d-vozovy-zvedak-hydraulicky-3-tuny-180-350-mm, accessed on 2021-07-26. (In Czech)
[16] Industrial Amplifier, from www.hbm.cz/wp-content/uploads/b0615.pdf, accessed on 2021-03-18.